Journal of Sound and Vibration (2001) **244**(1), 137–153
doi:10.1006/jsvi.2000.3461, available online at http://www.idealibrary.com on IDEAL®

THE LOCATION OF SPRING SUPPORTS FROM MEASURED VIBRATION DATA

J. K. SINHA† AND M. I. FRISWELL

Department of Mechanical Engineering, University of Wales Swansea, Singleton Park, Swansea SA2 8PP, Wales, U.K. E-mail: m.i.friswell@swansea.ac.uk

(*Received* 10 *May* 2000, *and in final form* 26 *October* 2000)

Detecting the position of supports within an elastic structure has many applications, particularly when these supports are not fixed. Previous studies have presented methods for the detection of translational support locations in elastic structures based on the minimization of the difference between the measured and computed natural frequencies. However, these discrete supports were constrained to be at nodes of the finite element model of the elastic structure. This required a fine mesh and the numerical computation of the eigenvalue derivative with respect to the support location. This paper has the same purpose, namely to identify the support locations, but the position of the supports is now a continuous parameter. When the support is located within an element the shape functions are used to produce the global stiffness matrix. The advantage is that the support location now appears explicitly in the formulation of the problem, and hence the analytical computation of the eigenvalue derivative is possible. Furthermore, the mesh may be much more coarse, requiring fewer degrees of freedom to detect the support locations, with reduced computational effort. The effect of identifying both the support stiffness and location is also discussed. The proposed approach has been illustrated with simulated and experimental examples used in the earlier studies.

1. INTRODUCTION

Many flexible mechanical systems such as fuel pins, heat exchanger tubes, control rods and various instrumented and shrouded tubes used in nuclear power plants and other engineering industries are beam-like components with a number of intermediate supports along their length. In many cases, these intermediate supports are firmly fixed. However, in some cases they may be loosely coupled and may move from their original locations during operation, for example because of flow-induced vibration. The movement of the supports may or may not affect the support stiffnesses depending upon the structural configuration. Undetected, such dislocated supports may deteriorate the system performance and consequently jeopardize the safety of the structure or plant. Visual inspection of such support locations in the structural system is not always possible if the structural configuration is complex. Other feasible inspection methods can be expensive and time consuming and may require the extended shutdown of the plant. Hence, a non-intrusive and non-destructive method for the detection of support locations in the structural system in a quick but reliable manner is important.

†Permanent address: Scientific Officer, Vibration Laboratory, Reactor Engineering Division, Bhabha Atomic Research Centre, Mumbai 400 085, India. E-mail: vilred@magnum.barc.ernet.in

0022-460X/01/260137 + 17 $35.00/0

Sinha *et al.* [1] presented a technique to locate simple massless translational spring supports in elastic structures, based on the measured natural frequencies of the structure. A gradient-based finite element (FE) model updating technique [2] was used based on a correlated FE model. The method involves the detection of spring support locations by updating the position of the support in the FE model through the minimization of the difference between measured and computed natural frequencies. This cost function is a highly non-linear function with respect to the updating parameters, and an iterative solution by a gradient search technique is used. Such an approach requires the formulation and computation of the sensitivity matrix (first order derivatives) of the cost function with respect to the updating parameters. Sinha *et al.* [1] used the support locations as updating parameters, but only allowed the supporting springs to be attached at nodes of the FE models of the beams. Therefore, the system mass and stiffness matrices, and thus the eigenvalues, were not a continuous function of the updating parameters. This lack of continuity meant that the eigenvalue derivatives and the sensitivity matrix could not be computed analytically, and had to be estimated numerically [1]. This method was used for solving typical problems encountered in nuclear power plants and was also tested on a small laboratory set-up [3]. Although the method was successful, if the actual location of the support is between two nodes of the FE model, it can only approximate this location to the nearest node. Hence, a very fine FE mesh is required to avoid large errors in the location of the supports, which requires a large computational effort.

This paper estimates the support locations in a similar manner, except now the spring location is a continuous parameter. If a spring is estimated to be attached within any element, then the shape functions of the beam element are used to approximate the extension in the spring. Now the support positions appear explicitly in the stiffness matrix, which is a continuous function of these updating parameters. The eigenvalue derivative with respect to the updating parameters, and hence the sensitivity matrix, may now be calculated analytically. The advantages gained compared to the earlier studies [1, 3] are as follows:

(1) an FE model with fewer degrees of freedom (d.o.f.s) may be used;
(2) supports can be detected at their exact physical location;
(3) eigenvalue derivatives may be computed analytically; and
(4) a significant reduction in computational effort is obtained.

This paper presents the theoretical formulation for estimating support location, including the FE modelling of the problem and the validation of the method through the simulated and experimental examples cited in the earlier studies [1, 3].

2. THEORETICAL FORMULATION

The problem of two simple beams with a number of massless intermediate spring supports is considered, as shown in the schematic diagram in Figure 1. It is assumed that the support springs move along the beam length and that this movement does not change their own stiffnesses. The spring locations are estimated using the gradient-based model updating method [2].

2.1. FE MODELLING

The FE model of the assembly is shown in Figure 2. The two-node Euler–Bernoulli beam element was used to model both beams, labelled A and B, and only bending in a single plane

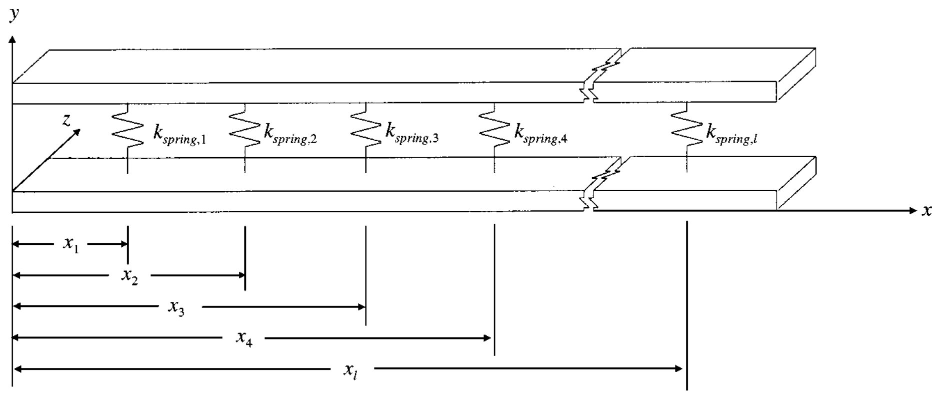

Figure 1. Schematic of two beams with interconnected intermediate supports. $k_{spring\ 1}, k_{spring,2}, \ldots, k_{spring,l} = 1$ Stiffnesses of firstr to lth supports.

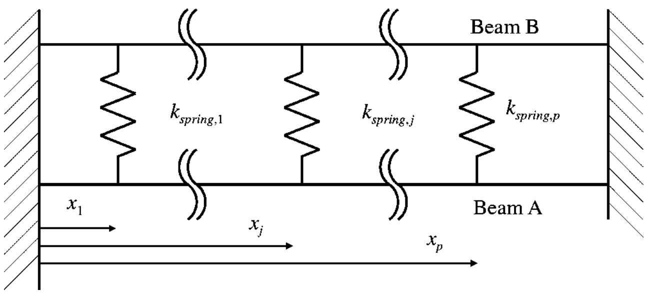

Figure 2. Beam models used.

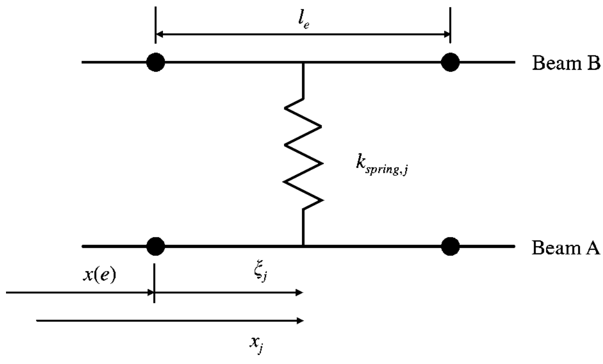

Figure 3. Modelling of the jth support spring.

is considered. A lumped mass matrix is used here, although there is no problem using a consistent mass matrix. Each node has two degrees of freedom, namely the translational displacement and bending rotation. The supports are modelled as springs (of stiffness k_{spring}), that may be placed within the beam elements of the FE model (see Figure 2). To aid understanding, the modelling procedure will be outlined for only one support (i.e., the jth support of spring stiffness, $k_{spring,j}$) between beams A and B, as shown in Figure 3. Within the eth element of beam A, the displacement is approximated (for Euler-Bernoulli beam theory) as

$$w_{eA}(\xi,t) = [N_{e1}(\xi)\ \ N_{e2}(\xi)\ \ N_{e3}(\xi)\ \ N_{e4}(\xi)] \begin{Bmatrix} w_{eA1}(t) \\ w_{eA2}(t) \\ w_{eA3}(t) \\ w_{eA4}(t) \end{Bmatrix} = N_e(\xi) \begin{Bmatrix} w_{eA1}(t) \\ w_{eA2}(t) \\ w_{eA3}(t) \\ w_{eA4}(t) \end{Bmatrix}, \tag{1}$$

where the shape functions, $N_{ei}(\xi)$, are

$$N_{e1}(\xi) = \left(1 - 3\frac{\xi^2}{l_e^2} + 2\frac{\xi^2}{l_e^3}\right), \quad N_{e2}(\xi) = l_e\left(\frac{\xi}{l_e} - 2\frac{\xi^2}{l_e^2} + \frac{\xi^2}{l_e^3}\right),$$

$$N_{e3}(\xi) = \left(3\frac{\xi^2}{l_e^2} - 2\frac{\xi^2}{l_e^3}\right), \quad N_{e4}(\xi) = l_e\left(-\frac{\xi}{l_e^2} + \frac{\xi^3}{l_e^3}\right). \tag{2}$$

Exactly the same shape functions and displacement approximation occur for each beam (but of course the nodal deflections will be different). If the support is at local position ξ_j then the strain energy in the spring support between beams A and B is

$$U = \tfrac{1}{2}\, k_{spring,j}(w_{eA}(\xi_j) - w_{eB}(\xi_j))^2, \tag{3}$$

where w_{eA} is the displacement of beam A, and similarly w_{eB} for beam B. Substituting equation (1), and the equivalent for beam B, into equation (3), gives the (8×8) local stiffness matrix (between the degrees of freedom at the nodes of the elements on both beams) as

$$\mathbf{K}_S = k_{spring,j} \begin{bmatrix} \mathbf{N}(\xi_j)^{\mathrm{T}}\mathbf{N}(\xi_j) & -\mathbf{N}(\xi_j)^{\mathrm{T}}\mathbf{N}(\xi_j) \\ -\mathbf{N}(\xi_j)^{\mathrm{T}}\mathbf{N}(\xi_j) & \mathbf{N}(\xi_j)^{\mathrm{T}}\mathbf{N}(\xi_j) \end{bmatrix}. \tag{4}$$

Similarly, the stiffness matrix $\mathbf{K}_S$ can be constructed for other supports. The stiffness matrices of the beams and the spring may be partitioned into those degrees of freedom affected by the spring stiffness, and the other degrees of freedom within the beam. Thus,

$$\mathbf{K}_A = \begin{bmatrix} \mathbf{K}_{A,II} & \mathbf{K}_{A,IS} \\ \mathbf{K}_{A,SI} & \mathbf{K}_{A,SS} \end{bmatrix} \quad \text{for beam A,} \tag{5}$$

$$\mathbf{K}_B = \begin{bmatrix} \mathbf{K}_{B,II} & \mathbf{K}_{B,IS} \\ \mathbf{K}_{B,SI} & \mathbf{K}_{B,SS} \end{bmatrix} \quad \text{for beam B,} \tag{6}$$

$$\mathbf{K}_S = \begin{bmatrix} \mathbf{K}_{S,AA} & \mathbf{K}_{S,AB} \\ \mathbf{K}_{S,BA} & \mathbf{K}_{S,BB} \end{bmatrix} \quad \text{for the supports.} \tag{7}$$

The stiffness matrices of the three substructures are partitioned into their internal and connected d.o.f. The first subscript A, B and S relates to beam A, beam B and the supports respectively. In the second and third subscripts, I represents the internal d.o.f. of the beams

A and B, depending upon the first subscript, and S represents the d.o.f. of the supports. The lumped mass matrix of beams A and B may be written in a similar fashion to stiffness matrix.

Using equations (5)–(7), the system eigenvalue equation is

$$\begin{bmatrix} \mathbf{K}_{A,II} & \mathbf{K}_{A,IS} & \mathbf{0} & \mathbf{0} \\ \mathbf{K}_{A,SI} & \mathbf{K}_{A,SS}+\mathbf{K}_{S,AA} & \mathbf{0} & \mathbf{K}_{S,AB} \\ \mathbf{0} & \mathbf{0} & \mathbf{K}_{B,II} & \mathbf{K}_{B,IS} \\ \mathbf{0} & \mathbf{K}_{S,BA} & \mathbf{K}_{B,SI} & \mathbf{K}_{B,SS}+\mathbf{K}_{S,BB} \end{bmatrix} \begin{Bmatrix} \boldsymbol{\phi}_{A,I} \\ \boldsymbol{\phi}_{A,S} \\ \boldsymbol{\phi}_{B,I} \\ \boldsymbol{\phi}_{B,S} \end{Bmatrix}$$

$$= \lambda \begin{bmatrix} \mathbf{M}_{A,II} & \mathbf{0} & \mathbf{0} & \mathbf{0} \\ \mathbf{0} & \mathbf{M}_{A,IS} & \mathbf{0} & \mathbf{0} \\ \mathbf{0} & \mathbf{0} & \mathbf{M}_{B,II} & \mathbf{0} \\ \mathbf{0} & \mathbf{0} & \mathbf{0} & \mathbf{M}_{B,SI} \end{bmatrix} \begin{Bmatrix} \boldsymbol{\phi}_{A,I} \\ \boldsymbol{\phi}_{A,S} \\ \boldsymbol{\phi}_{B,I} \\ \boldsymbol{\phi}_{B,S} \end{Bmatrix} \tag{8}$$

or,

$$\mathbf{K}\boldsymbol{\phi} = \lambda \mathbf{M}\boldsymbol{\phi}, \tag{9}$$

where $\mathbf{K}$ and $\mathbf{M}$ are the system stiffness and mass matrices and $\boldsymbol{\phi}$ is the normalized eigenvector of the structural system and λ is the eigenvalue.

2.2. ESTIMATION OF SUPPORT LOCATIONS

One of the gradient-based model updating methods, namely the *Penalty Function method* [2], based on natural frequencies only, is used to estimate the support locations. The vector of updating parameters, $\boldsymbol{\theta} = [x_1, x_2, \ldots, x_p]^{\mathrm{T}}$, consists of the locations of the p supports, measured from one end of the beams. If required, the support stiffnesses may also be included as unknown parameters. These parameters will not be considered further in this section because the use of such parameters in model updating is common, and their inclusion is straightforward [2]. The first m eigenvalues (natural frequency squared) are measured and placed in the measurement vector, $\mathbf{z}_e = [\lambda_{e1}, \lambda_{e2}, \ldots, \lambda_{em}]^{\mathrm{T}}$. The corresponding eigenvalues computed from the FE model are $\mathbf{z}_c = [\lambda_{c1}, \lambda_{c2}, \ldots, \lambda_{cm}]^{\mathrm{T}}$. Mode shapes (or eigenvectors) may also be included in the measurement vector, although this is a minor extension to the approach, and is not considered further.

The eigenvalues may be written as a first order truncated Taylor series expansion in terms of the updating parameters, giving the error vector, $\boldsymbol{\varepsilon}$, as

$$\boldsymbol{\varepsilon} = \delta\mathbf{z} - \mathbf{S}\,\delta\boldsymbol{\theta}, \tag{10}$$

where $\delta\boldsymbol{\theta}$ is the vector of perturbations in the support locations and $\delta\mathbf{z} = \mathbf{z}_e - \mathbf{z}_c$ is the eigenvalue error. Note that it is important that the correct modes are paired, which is conveniently checked using the modal assurance criteria (MAC) [4]. The sensitivity matrix, $\mathbf{S}$, is the first derivative of eigenvalues with respect to the support locations,

$$\mathbf{S} = \begin{bmatrix} \frac{\partial \lambda_{c1}}{\partial x_1} & \frac{\partial \lambda_{c1}}{\partial x_2} & \cdots & \frac{\partial \lambda_{c1}}{\partial x_p} \\ \frac{\partial \lambda_{c2}}{\partial x_1} & \frac{\partial \lambda_{c2}}{\partial x_2} & \cdots & \frac{\partial \lambda_{c2}}{\partial x_p} \\ \vdots & \vdots & \ddots & \vdots \\ \frac{\partial \lambda_{cm}}{\partial x_1} & \frac{\partial \lambda_{cm}}{\partial x_2} & \cdots & \frac{\partial \lambda_{cm}}{\partial x_p} \end{bmatrix}. \tag{11}$$

The derivatives in equation (11) are computed [5] as

$$\frac{\partial \lambda_{ci}}{\partial x_j} = \boldsymbol{\phi}_i^{\mathrm{T}} \left[\frac{\partial \mathbf{K}}{\partial x_j} - \lambda_{ci} \frac{\partial \mathbf{M}}{\partial x_j} \right] \boldsymbol{\phi}_i, \tag{12}$$

where λ_{ci} and $\boldsymbol{\phi}_i$ are the ith eigenvalue and eigenvector. In the estimation of spring support locations, the derivative $\partial \mathbf{M}/\partial x_j$ is zero since the mass of the spring supports is assumed to be negligible. The derivative $\partial \mathbf{K}/\partial x_j$ is computed by differentiating the system stiffness matrix (equation (8)).

The position of the jth support at the end of each iteration is given by x_j. Suppose that the jth support is placed within the eth element of beam A (see Figure 3). Then,

$$x_j = x(e) + \xi_j, \tag{13}$$

where $x(e)$ is the position of the eth node and ξ_j is the local co-ordinate of the jth support in the eth element. Since $x(e)$ is fixed, $\partial \mathbf{K}/\partial x_j = \partial \mathbf{K}/\partial \xi_j$, and hence equation (12) becomes

$$\frac{\partial \lambda_{ci}}{\partial x_j} = \frac{\partial \lambda_{ci}}{\partial \xi_j} = \boldsymbol{\phi}_i^{\mathrm{T}} \frac{\partial \mathbf{K}}{\partial \xi_j} \boldsymbol{\phi}_i. \tag{14}$$

Only coefficients of the spring support stiffness matrix $\mathbf{K}_S$ depend on the local co-ordinate, ξ. Thus,

$$\frac{\partial \lambda_{ci}}{\partial \xi_j} = \boldsymbol{\phi}_i^{\mathrm{T}} \begin{bmatrix} \mathbf{0} & \mathbf{0} & \mathbf{0} & \mathbf{0} \\ \mathbf{0} & \frac{\partial \mathbf{K}_{S,AA}}{\partial \xi_j} & \mathbf{0} & \frac{\partial \mathbf{K}_{S,AB}}{\partial \xi_j} \\ \mathbf{0} & \mathbf{0} & \mathbf{0} & \mathbf{0} \\ \mathbf{0} & \frac{\partial \mathbf{K}_{S,BA}}{\partial \xi_j} & \mathbf{0} & \frac{\partial \mathbf{K}_{S,BB}}{\partial \xi_j} \end{bmatrix} \boldsymbol{\phi}_i. \tag{15}$$

It is vital that the eigenvalue derivative should be continuous at the nodes of the FE model. If the spring support is located at a node, either of the elements connected to this node may be used to determine the eigenvalue derivative, and both these derivatives must be equal. The derivative of the support stiffness matrix, equation (4), consists of terms like

$$\frac{\partial}{\partial \xi_j} [\mathbf{N}(\xi_j)^{\mathrm{T}} \mathbf{N}(\xi_j)] = \mathbf{N}'(\xi_j)^{\mathrm{T}} \mathbf{N}(\xi_j) + \mathbf{N}(\xi_j)^{\mathrm{T}} \mathbf{N}'(\xi_j). \tag{16}$$

However, evaluating this expression at the ends of the elements gives, from equation (2),

$$\left.\frac{\partial \mathbf{N}^{\mathrm{T}}\mathbf{N}}{\partial \xi_j}\right|_{\xi_j=0} = \begin{bmatrix} 0 & 1 & 0 & 0 \\ 1 & 0 & 0 & 0 \\ 0 & 0 & 0 & 0 \\ 0 & 0 & 0 & 0 \end{bmatrix} \quad \text{and} \quad \left.\frac{\partial \mathbf{N}^{\mathrm{T}}\mathbf{N}}{\partial \xi_j}\right|_{\xi_j=l_e} = \begin{bmatrix} 0 & 0 & 0 & 0 \\ 0 & 0 & 0 & 0 \\ 0 & 0 & 0 & 1 \\ 0 & 0 & 1 & 0 \end{bmatrix}. \tag{17}$$

Although these look different, when these expressions are substituted into equations (4) and (12) the non-zero terms pick out the same d.o.f.s in the eigenvector. Thus, the eigenvalue derivatives are continuous at the nodes.

The penalty function, $\mathbf{J}$, is formed as [2]

$$\mathbf{J}(\delta\boldsymbol{\theta}) = \boldsymbol{\varepsilon}^{\mathrm{T}}\mathbf{W}_{\varepsilon}\boldsymbol{\varepsilon}, \tag{18}$$

where $\mathbf{W}_{\varepsilon}$ is the positive diagonal weighting matrix which reflects the confidence level in the frequency measurements. It is generally taken as the reciprocal of the variance (the square of the standard deviation) of the corresponding measurements [2].

The vector of desired support locations can be obtained by minimizing $\mathbf{J}$ with respect to $\delta\boldsymbol{\theta}$ which involves the differentiation of $\mathbf{J}$ with respect to each parameter, and setting the result equal to zero. The perturbation in the parameter vector is then

$$\delta\boldsymbol{\theta} = [\mathbf{S}^{\mathrm{T}}\mathbf{W}_{\varepsilon}\mathbf{S}]^{-1}\,\mathbf{S}^{\mathrm{T}}\mathbf{W}_{\varepsilon}\,\delta\mathbf{z}. \tag{19}$$

Since equation (10) is a linear approximation, the method is iterative. A new model with the updated support locations is generated, and the revised analytical eigenvalues and sensitivity matrix are produced. The iteration process continues until the solution converges.

2.3. COMPUTATIONAL IMPLEMENTATION

To implement the above formulation (equation (19)) for the estimation of support locations, the modal data need to be computed for a given set of support locations $\boldsymbol{\theta}$. In this paper, an FE model is used for this purpose. In addition, experimental modal data measured on a structure with unknown support locations are required to determine $\delta\mathbf{z}$. The iterative process in equation (19) requires an initial guess for the support locations. After each iteration, the updated values of the support locations, for example x_j of the jth support, is compared to nearby nodal position of the FE model in order to place the jth support within the correct element of the FE model. The matrices for the two beams do not have to be generated at each iteration. Only the stiffness matrix of the spring supports have to be computed, and placed in the correct positions in the global stiffness matrix. Note that equation (8) implies that the ordering of d.o.f. changes if the location of the supports changes from one element to another. In practice, the ordering of the d.o.f. would be fixed, and the spring support stiffness matrix would be placed at the correct d.o.f.s.

No mention has been made of regularization or conditioning of the estimation procedure [6]. One advantage of specifying the position of the support, rather than estimate stiffness values for all elements, is that the number of parameters is reduced. In general, the fewer the parameters that need to be estimated the better is the conditioning of the problem. If natural frequencies are used, then the number of modes measured must be equal to, or preferably larger than, the number of support locations. If the support stiffnesses are also estimated then there must be twice as many modes as supports. However, ensuring that there are more measurements than parameters does not guarantee a well-conditioned problem, as different parameters may have a similar effect on the predicted eigenvalues. This does not appear to be a problem in the examples below, partly because only one or two supports are identified. The effect of location and stiffness are likely to be different, since the support location is likely to affect different modes in different ways, whereas the support stiffness is likely to change all the modes in a similar way.

3. SIMULATED AND EXPERIMENTAL EXAMPLES

To determine the spring support locations, measured modal data and an initial estimate of the locations are required. The measured data required consist of measured natural frequencies and mode shapes of the structure corresponding to some support locations that are to be determined. This set of data is henceforth referred to as the target data for the iterative solution. In the examples given only the natural frequencies are used in the estimation. Any of the well-known experimental techniques for modal analysis [7] can be used to obtain these modal parameters. In the numerical study, simulated modal data are used in place of the experimental modal data for the assessment of the method. To determine the effectiveness of the present formulations in comparison with earlier studies [1, 3] the same examples are used. Examples 1, 3 and 4 assume that the support stiffness is known accurately. If this is not the case then these support stiffnesses should also be estimated, and this is the purpose of examples 2 and 5.

3.1. EXAMPLE 1: NUMERICAL SIMULATION OF PARALLEL BEAMS

The problem of two fixed–fixed beams of different dimensions with two spring supports of stiffness 10 kN/m was considered first [1]. Both beams were 2 m long, and beams A and B had cross-sections 50×25 mm and $25 \times 12{\cdot}5$ mm respectively. The Young's modulus of elasticity and the density for both beams were 70 GN/m^2 and 2666·67 kg/m^3 respectively.

TABLE 1

The location of two unsymmetrically placed spring supports between two beams

		Case 1a		Case 1b		Case 1c	
Parameters		Initial	Target	Initial	Target	Initial	Target
Support x_1 (mm)		520·0	440·0	520·0	440·0	520·0	440·0
Location x_2 (mm)		1880·0	1720·0	1880·0	1400·0	1880·0	1200·0
Natural frequencies (Hz)		19·217	18·771	19·217	22·091	19·217	24·344
		33·295	33·252	33·295	34·107	33·295	35·232
		48·950	48·991	48·950	51·487	48·950	49·544
Iterations required	Present study—(76 d.o.f.)	05		08		07	
	Earlier study—(196 d.o.f.) [1]	05		06		09	

TABLE 2(a)

The location of two symmetrically placed spring supports between two beams

Parameters		Case 1d Initial	Case 1d Target	Case 1e Initial	Case 1e Target	Case 1f Initial	Case 1f Target
Support location	x_1 (mm)	520·0	240·0	520·0	280·0	520·0	360.0
	x_2 (mm)	1880·0	1760·0	1880·0	1720·0	1880·0	1640·0
Natural frequencies (Hz)		19·217	17·041	19·217	17·428	19·217	18·565
		33·295	32·986	33·295	33·040	33·295	33·221
		48·950	46·542	48·950	47·211	48·950	48·885
Iterations required	Present study—(76 d.o.f.)	14		12		13	
	Earlier study—(196 d.o.f.) [1]	08		15		05	

TABLE 2(b)

The location of two symmetrically placed spring supports between two beams

Parameters		Case 1g Initial	Case 1g Target	Case 1h Initial	Case 1h Target	Case 1i Initial	Case 1i Target
Support location	x_1 (mm)	520·0	440·0	520·0	600·0	520·0	800·0
	x_2 (mm)	1880·0	1560·0	1880·0	1400·0	1880·0	1200·0
Natural frequencies (Hz)		19·217	20·139	19·217	23·853	19·217	26·699
		33·295	33·548	33·.295	34·935	33·295	37·785
		48·950	50·634	48·950	52·150	48·950	48·651
Iterations required	Present study—(76 d.o.f.)	10		14		13	
	Earlier study—(196 d.o.f.) [1]	09		07		14	

Both of the beams were divided into 20 elements of equal length, giving a total of 76 d.o.f. The number of d.o.f. used was less than 40% of those used in the earlier study [1]. The support locations, x_1 and x_2, for both the spring supports were chosen as updating parameters.

Many exercises were carried out to determine the location of both the spring supports for different target data from a variety of initial guesses. The measured data consisted of the first three eigenvalues, and the weighting matrix was taken as the identity. Tables 1 and 2 show the results of these exercises, and show that the support locations were successfully identified without any error. The results of the earlier study are also listed in the tables for comparison. Figure 4 shows the convergence of the parameters for case 1i. As expected,

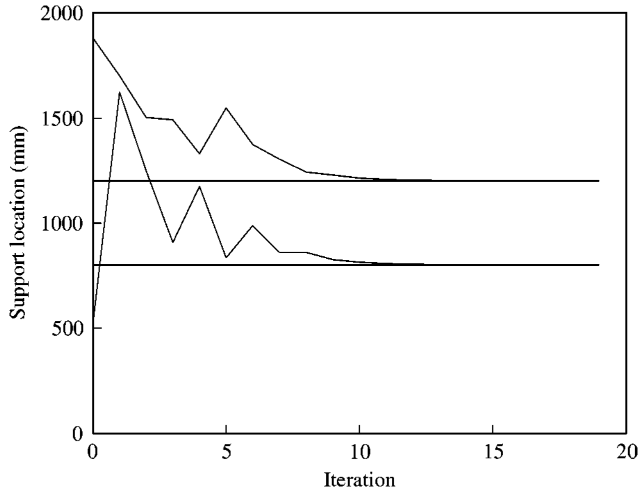

Figure 4. Convergence of the two estimated support locations for case 1i.

since the example does not include any noise or errors, the updated support locations exactly match the target locations.

3.2. EXAMPLE 2: NUMERICAL SIMULATION OF PARALLEL BEAMS—IDENTIFICATION OF SUPPORT LOCATION AND STIFFNESS

The above example was now repeated, except that the support stiffness was also identified, along with the location. Since only three natural frequencies are assumed to be measured, only one support location and stiffness can be identified. Table 3 shows the results of these exercises, and shows that the support locations are successfully identified without any error. Figure 5 shows the convergence of the parameters for cases 2a and 2e. As expected, since the example did not include any noise or errors, the updated support location and stiffness exactly match the target data.

3.3. EXAMPLE 3: NUMERICAL SIMULATION OF COAXIAL TUBES

The second system was also a numerical simulation, in this case two coaxial tubes with two loosely held spacers maintaining the annular gap between the tubes [3]. Figure 6 shows a schematic of the tube assembly. Both tubes were 6350 mm long, and tube A had a diameter and thickness of 100 mm and 5 mm and tube B had a diameter and thickness of 150 mm and 2 mm. The Young's modulus and the mass density for the tubes were 200 GN/m^2 and 8000 kg/m^3 respectively. The ends of both the tubes were fixed. The stiffness of both the massless spacers was 1 GN/m. Both tubes were discretized into 31 Euler–Bernoulli beam elements, giving a total of 62 elements and 120 d.o.f. The number of d.o.f. used was less than 25% of those used in the earlier study [3].

Once again, the two spacer locations, x_1 and x_2, were chosen as the updating parameters, and Table 4 gives the results of estimated spacer locations. Clearly, the spacers were located correctly in fewer iterations than in the earlier study [3]. Figure 7 shows the convergence of the support locations case 3a.

TABLE 3(a)

The estimation of the stiffness and location of a spring support between two beams

	Case 2a		Case 2b		Case 2c	
Parameters	Initial	Target	Initial	Target	Initial	Target
Support location, x_1 (mm)	520·0	240·0	520·0	600·0	520·0	740·0
Support stiffness, $k_{spring,1}$ (N/m)	11 300	10 600	11 300	11 500	11 300	11 850
Natural frequencies (Hz)	19·434 33·332 49·339	16·764 32·954 45·991	19·434 33·332 49·339	20·601 33·559 49·864	19·434 33·332 49·339	22·743 34·196 49·032
No. of iterations required	05		03		06	

TABLE 3(b)

The estimation of the stiffness and location of a spring support between two beams

	Case 2d		Case 2e	
Parameters	Initial	Target	Initial	Target
Support location, x_1 (mm)	520·0	850·0	520·0	950·0
Support stiffness, $k_{spring,1}$ (N/m)	11 300	12 125	11 300	12 375
Natural frequencies (Hz)	19·434 33·332 49·339	24·183 34·973 47·113	19·434 33·332 49·339	24·973 35·674 45·604
No. of iterations required	19		08	

3.4. EXAMPLE 4: LABORATORY-SCALE EXPERIMENT

The last system was a laboratory-scale experiment that consisted of two tubes made of steel which were inter-connected by a rubber band [3]. The schematic of the set-up is shown in Figure 8(a). The detail of the dimensions and the boundary conditions of both the tubes are also marked in the figure. A modal test was carried out using impact excitation [7]. It was assumed that the spring action of the rubber band was linear for the small levels of excitation used in the test. Modal tests were conducted for two different locations of the rubber band (656·5 and 746·5 mm from one end), and the identified natural frequencies are listed in Table 5. Figure 8(b) shows the FE model of the set-up that was developed using lumped mass Euler–Bernoulli beam elements for both the tubes and a spring element for the rubber band. A total of 96 d.o.f. (46 translation d.o.f. and 50 rotational d.o.f.) were used in the FE model, which is 39% of the number used previously [3]. The stiffness of the elastic band was measured as 0·9278 N/m.

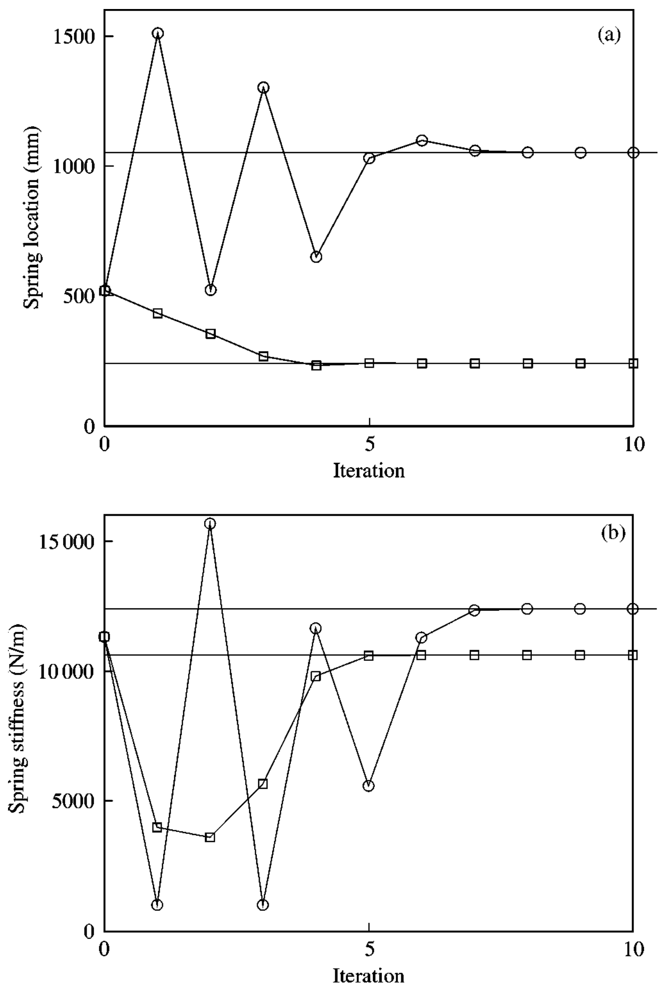

Figure 5. Convergence of the estimated parameters for cases 2a (□-□-□) and 2e (○-○-○): (a) Location estimation; (b) stiffness estimation.

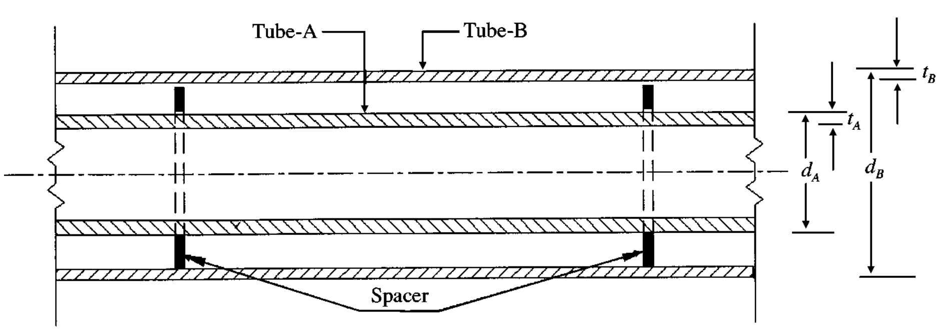

Figure 6. Schematic of the assembly of two coaxial tubes.

The location of the spring was carried out using the position of the spring, x_1, as the updating parameter. As shown in Table 5 the target location for both cases was detected at the fifth iteration from the initial guess of the rubber spring at 508 mm. The position of the spring for both cases had a very small error of less than 1% of the target locations. Thus, an

TABLE 4

The location of two spacers between a twin coaxial tube assembly

		Case 3a		Case 3b		Case 3c	
Parameters		Initial	Target	Initial	Target	Initial	Target
Support location	x_1 (mm)	2450·0	2950·0	2450·0	2350·0	2450·0	2850·0
	x_2 (mm)	4350·0	3950·0	4350·0	3850·0	4350·0	3350·0
Natural frequencies (Hz)		18·723	18·705	18·723	18·725	18·723	18·687
		50·923	49·614	50·923	50·755	50·923	49·147
		80·104	72·292	80·104	80·128	80·104	71·081
Iterations required	Present study—(120 d.o.f.)	10		05		19	
	Earlier study—(504 d.o.f.) [3]	14		06		19	

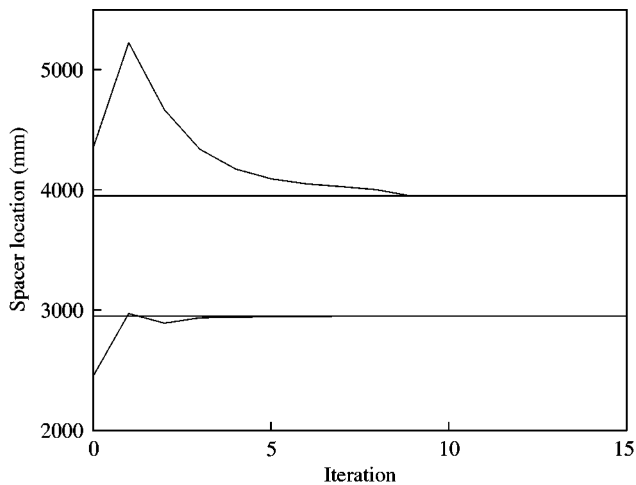

Figure 7. Convergence of the two estimated support locations for case 3a.

FE model with a small number of d.o.f. was sufficient to determine the support locations correctly. Figure 9 shows the convergence of the support locations.

3.5. EXAMPLE 5: LABORATORY-SCALE EXPERIMENT—IDENTIFICATION OF SUPPORT LOCATION AND STIFFNESS

The above example was now repeated, except that the support stiffness was also identified, along with the location. Table 6 shows the results of the identification, and Figure 10 shows the convergence of the parameters. The location of the spring was identified with an error of 5·11 and 0·39% for the two cases. The error in the estimated spring stiffness was larger, at 20·0 and 2·65% from the target stiffness of 0·9278 N/m.

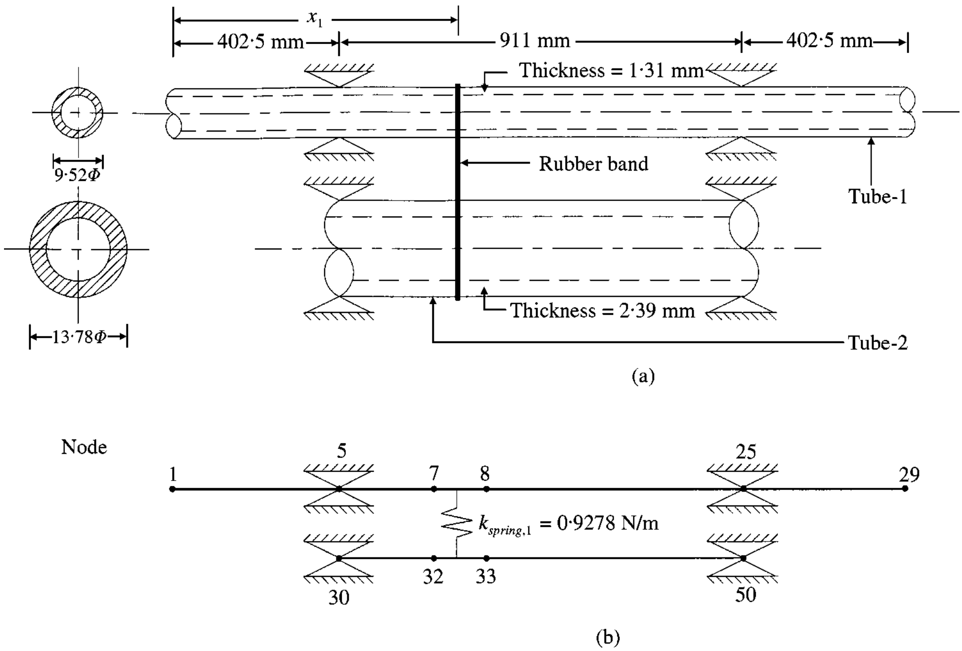

Figure 8. Laboratory experimental set-up: (a) schematic of the set-up assembly; (b) FE model.

TABLE 5

The location of a rubber band spring between two tubes for the experimental example

Parameters		Case 4a Initial	Case 4a Test data	Case 4b Initial	Case 4b Test data
Support location, x_1 (mm)		508·44	656·50	508·44	746·50
Natural frequencies (Hz)		18·053 29·081 37·219	20·938 28·750 39·375	18·053 29·081 37·219	21·875 29·375 39·375
Present study— (96 d.o.f.)	Estimated location	651·97 mm	(−0·69%)	745·05 mm	(−0·19%)
	No. iterations	05		05	
Earlier study [3]— (248 d.o.f.)	Estimated location	656·74 mm	(0·04%)	741·48 mm	(−0.67%)
	No. iterations	03		04	

Figure 10 clearly shows that the conditioning of the estimation problem was worse, and convergence was slower, than when only the location was estimated. One reason for this was that the spring stiffness was relatively small, and the difference in the natural frequency for stiffness values of 0·7421 and 0·9278 N/m was very small. However, it was gratifying that

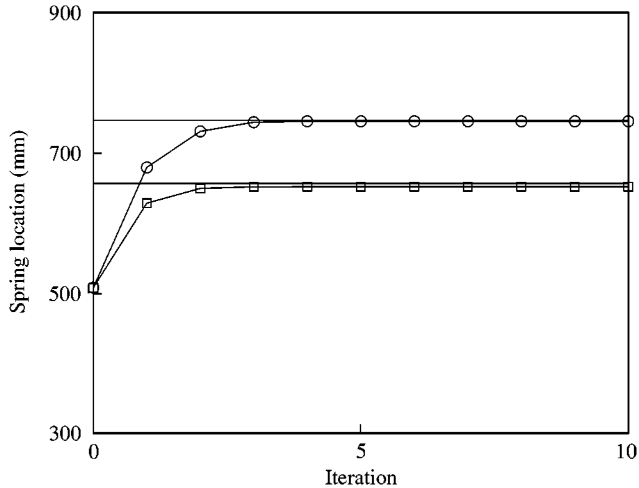

Figure 9. Convergence of the estimated support location for cases 4a (□-□-□) and 4b (○-○-○).

TABLE 6

The estimation of the stiffness and location of a rubber band spring between two tubes for the experimental example

	Case 5a			Case 5b		
	Initial	Test data	Estimated	Initial	Test data	Estimated
Support location, x_1 (mm)	508·44	656·50	690·08 (5·11%)	508·44	746·50	743·60 (− 0·39%)
Support stiffness, $k_{spring,1}$ (N/m)	2·00	0·9278	0·7421 (− 20.0%)	2·00	0·9278	0·9032 (− 2.65%)
Natural frequencies (Hz)	19·253 29·468 54·057	20·938 28·750 39·375	20·674 28·891 39·630	19·253 29·468 54·057	21·875 29·375 39·375	21·504 28·780 40·424
No. iterations		05			13	

the spring was located accurately, and the estimate of location seemed more robust to errors than the estimate of stiffness.

4. CONCLUDING REMARKS

A method for the estimation of the locations of interconnecting intermediate spring supports in beam structures as a solution of an inverse vibration problem has been presented. The methodology uses a baseline FE model along with the modal test data in a gradient-based model updating method. The changes in the natural frequency characteristics of the structural system due to the movement of the loosely held spring supports are used. The formulation presented in the paper is slightly more involved than

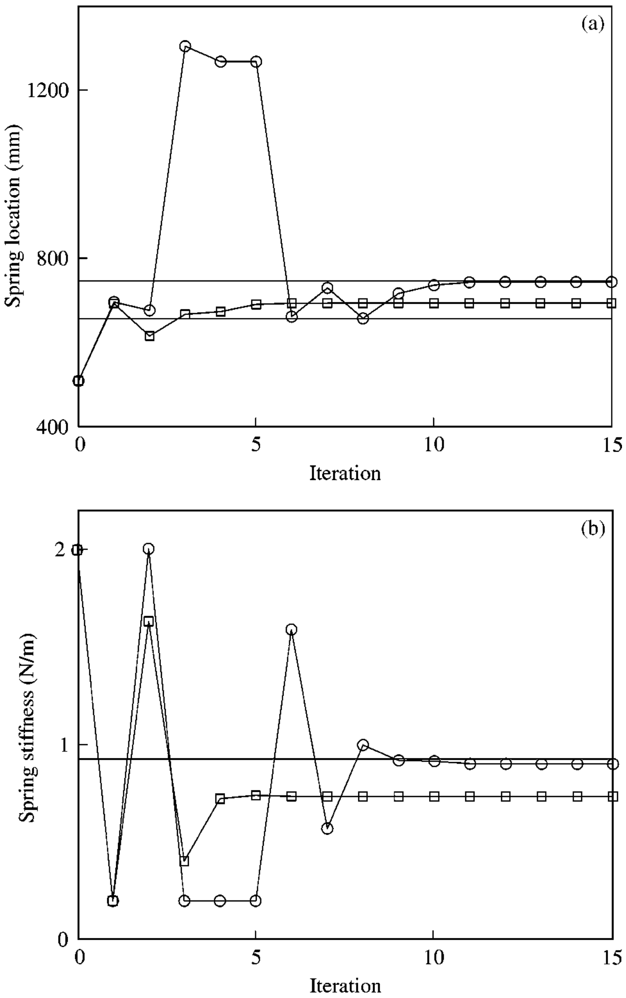

Figure 10. Convergence of the estimated parameters for cases 5a (□-□-□) and 5b (○-○-○): (a) location estimation; (b) stiffness estimation.

earlier studies. However, the advantage of the present formulation is that an FE model with far fewer d.o.f. is sufficient to locate the support accurately, and hence significantly reduces the computation required. Furthermore, in the proposed method the parameters are continuous, which avoids the complicated numerical estimate of the eigenvalue derivative required previously. The validation and the advantages of the proposed method have been highlighted through numerical simulations and an experimental example. In the illustrative examples, only one and two supports are used, although this is not a constraint of the method. Beam models have been used in the development of the method, although a similar approach for plate elements is possible.

ACKNOWLEDGMENTS

Jyoti K. Sinha acknowledges the support of the Department of Science and Technology, India through the award of a BOYSCAST Fellowship. Sinha also acknowledges the parent organization BARC, India for consistent support and encouragement. Michael Friswell acknowledges the support of the EPSRC through the award of an Advanced Fellowship.

REFERENCES

1. J. K. SINHA, P. M. MUJUMDAR and R. I. K. MOORTHY 2000 *Journal of Sound and Vibration* **240**, 499–518. Detection of spring support locations in elastic structures using gradient based finite element model updating technique.
2. M. I. FRISWELL and J. E. MOTTERSHEAD 1995 *Finite Element Model Updating in Structural Dynamics*, Dordrecht: Kluwer Academic Publishers.
3. J. K. SINHA, P. M. MUJUMDAR and R. I. K. MOORTHY 2000 *Nuclear Engineering and Design* **196**, 139–151. A parameter identification technique for detection of spacer locations in an assembly of two coaxial flexible tubes.
4. R. J. ALLEMANG and D. L. BROWN 1982 *First IMAC*, 110–116. A correlation coefficient for modal vector analysis.
5. R. L. FOX and M. P. KAPOOR 1968 *American Institute of Aeronautics and Astronautics Journal* **6**, 2426–2429. Rates of change of eigenvalues and eigenvectors.
6. M. I. FRISWELL, J. E. MOTTERSHEAD and H. AHMADIAN 2000 *Proceedings of the Royal Society of London, Series A: Mathematical, Physical and Engineering Sciences* **359**, 169–186. Finite element model updating using experimental test data: parameterisation and regularisation.
7. D. J. EWINS 1984 *Modal Testing: Theory and Practice*. Taunton, U.K.: Research Studies Press.